

Rolling Ball Detection for Signs in Aircraft Measurement

Wusheng Luo, Jingjing Xiao, Qin Lu, Pei Li

Department of Instrument Science and Technology, College of Mechatronics Engineering and Automation, National University of Defense Technology, Changsha 410073, China

Received: Apr. 8, 2012; Revised May. 4, 2012; Accepted Jun. 6, 2012

Abstract: The key problem of stereo vision in measurement is how to find the anchor signs of objects for matching. In this paper, we firstly propose the method of signs designing to describe the basic structures of aircraft. A novel algorithm called rolling ball is proposed to detect them. The method opens some detecting windows. Through computing the distance between weight center and the geometrical center of each window, the algorithm could capture the start pixels of the signs and find the raw moving vector. Adding the condition of original moving vector, the synthetical vector ensures that the signs track will not be affected by intersection. We could obtain more accurate detection results in terms of the restrictions of width, length and moving degrees. Both of the simulation and aircraft measurement experiments demonstrate that the method could find out the anchor signs automatically and correctly. In addition, we get some useful data which could be regarded as basic parameters when adopting the rolling ball method in stereo matching to detect the signs.

Keywords: Aircraft measurement, Information signs, Rolling ball detection.

1. Introduction

Aircraft measurement is quite important for researchers to find out the characters of planes. It can also help technician to control the aircraft, making aircraft escape out from some extremely dangerous situations like spin. The conventional way to estimate parameters of aircraft attitude was mainly based on manpower in wind tunnel [1] which will take quite a long time to finish it, approximately one week. In this method, people took photographs of the moving aircraft model in spin, then they put a smaller model (i.e. the same frame with spin model, only the size is smaller) to match the projection produced by photographs. When the smaller models attitude has the same projection as real aircraft, engineers could get the pose of the real spin model. During this process, the work accomplished by manpower will contain subjective errors inevitably, and the experimental data is insufficient for a higher precision requirement at times. In addition, the overall workload is unbelievable huge. With two aircraft models required in this method, the cost, which will be very high, has to be taken into account seriously.

Therefore, another measurement method based on stereo vision is used in the Langley 20-Foot Vertical Spin Tunnel in America [2-7]. Data for free-flying models are obtained

from up to four high-grade monochrome CCD video cameras which provide inputs into the dynamic model data acquisition system. These cameras provide 60-Hz imaging of retroreflective target that are precisely positioned on the surface of the model, and the poses of aircraft model are recognized by the retroreflective targets. In this method, the data processing is on the base of computer, and it takes much less time. The algorithm could obtain more data and avoid subjective errors effectively.

In recent years, a vertical wind tunnel has been built in China [8]. Because stereo vision could measure the aircraft efficiently; this method is widely used in such kind of scenes. The general processing of stereo vision measurement is divided into the following three steps:

- Camera calibration. This is an important step to get the inner parameters of cameras for computing.
- Stereo matching. It is to find out the corresponding points in different images.
- 3D recovery. Based on previous steps, we can compute the aircrafts pose in terms of geometric relationship in 3D space.

In these three steps, camera calibration is quite mature. Using the camera calibration toolbox provided by California institute for free sharing, we can obtain those significant

* Corresponding author: e-mail: shine636363@sina.com

parameters easily. Stereo matching is a complicated problem which largely draws researchers attention. After stereo matching, 3D recovery becomes a simple problem which benefits from the knowledge of the geometric relationship that could be got after the camera calibration and installation. However, if we recover the whole 3D information in stereo matching, it will cost large amount of computational time and make the stereo matching become extremely difficult. In addition, overall recovery is very sensitive to the noise. Using this method, the computed results are not stable enough. On the contrary, recovering the proper sparse 3D information also can obtain the measurement parameters, but it takes very little time. Moreover, it can decline the complexity of stereo matching. Therefore, sparse recovery method gradually catches the researchers interest [16].

One key step of stereo matching based on the sparse 3D information recovery is to seek the proper information points for recovery. Using these information points, we are able to know the basic structure of the aircrafts and compute their attitude due to the geometric relationships. Additionally, detection for these points should be quite easy and the signs will not cause any confusion. To measure up these requirements, our paper focuses on information points designing and proposes a novel detecting method to seek them, so that the stereo matching becomes much easier and faster. This can contribute to the aircraft measurement and ensure the computed results are reliable.

The main body of this paper is organized as follows. Section 2 states how to design and distribute the information points so that these signs are capable to describe the structure of planes and be easy to be detected. Section 3 details the rolling ball method to detect these character signs for stereo matching. The application and usefulness of the proposed algorithm are demonstrated in Section 4 by the method of simulation and applying it to the aircraft measurement. Finally, Section 5 draws detailed conclusions.

2. INFORMATION SIGNS

As described before, the overall information recovery will cost large amount of computational resources. We should find proper signs as anchor points for sparse stereo matching and recovery. Even though the structure of aircraft model is simple, so many edges and corners, which are parts of the model shapes, will cause confusion in computer vision and make correct recognitions very difficult (in Fig1). Thus, in this part, we will design proper signs so that they can describe the basic aircraft structure for measurement. In the meanwhile, these information signs should be able to make the detection become much easier.

The basic principles for signs making are stated as follows:

- The new signs must not bring too much additional weight to the aircraft or affect the experiment of the measurement.

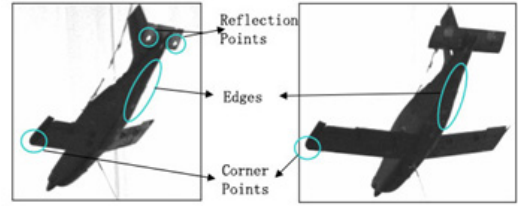


Figure 1 Different Poses of Aircraft

- The designed signs ought to be detected easily. This contains two meanings: Firstly, the signs could be anchored easily; Secondly, it takes very little time to find out them.
- Different signs could be classified easily in order to complete stereo matching. It means that the algorithm could confirm the location of signs in terms of their different shapes or sizes.

In relevant research, Domae [9] adopts the structure ray to make the characteristic points, but this method will add new optic equipment and it requires the objects staying statically, while it is impossible in aircraft measurement. A Canada company uses Optotrak technology which takes lighting marker points as signs [10]. However, the light-emitting diode (LED) will bring intolerant weight and the cost of this technology is very high. Erol [11] points out to use the man-made signs which is easy to be detected and will not bring additional weight, but in the paper it does not provide detailed information. Therefore, our research will base on Erol work and make a deeper study of this method.

2.1. Selection of the Man-made Signs

The widespread man-made signs are shown in the Fig.2. From the picture, we could find that (a) to (c) are basic signs and (d) to (i) are transfigurations of them. Signs from (j) to (o) are coding signs.

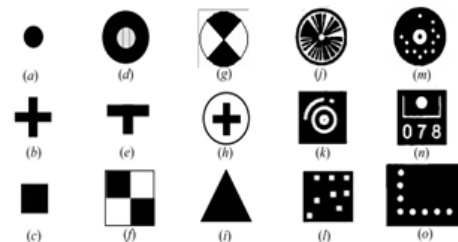


Figure 2 The Popular Man-made Signs

Noticeably, even though the coding signs are easy to be classified, in most cases these signs are very complex

to process and they should not endure too much distortion during stereo matching. However, the aircrafts have numerous poses in the measurement. The distortion is unavoidable so that we cannot use these kinds of signs. When we are doing experiments, the aircraft will cause some reflection areas(in Fig.1). The shapes of these areas are like rotundity and rectangle which will make confusion between reflection areas and attached signs if choosing Fig.2 (a) or (c) as the anchor signs. On the contrary, cross signs (b) are not sensitive to the distortion and will not be mistaken by reflection areas. Additionally, the clear intersection points of crosses make the signs be able to anchor their location precisely. Only when the planes with signs are approximately vertical for the image planes (Fig.3 (c)), the signs cannot be detected. However, this situation is very remote so that these signs will be used in our experiment.



Figure 3 The Experimental Effect of Cross Signs

2.2. Attachment of Man-made Signs

After selecting the proper shapes of signs, we are going to distribute these man-made signs on the suitable and meaningful location so that they are capable to describe the basic structure of aircraft and can be detected easily.

As we know, the attitude of aircraft is mainly decided by important parameters of the pitch angle θ and roll angle φ . In the Fig.4, the unit vector of $O_p X_p$ in aircraft coordinates is n_1 , while the unit vector of $O_p Y_p$ is n_2 . n_z represents the unit vector $O_w Z_w$ in the world coordinates. Then, we could compute pitch angle θ by (1):

$$\theta = \arccos(n_2 \cdot n_z) - \frac{\pi}{2} \tag{1}$$

And the roll angle φ by (2):

$$\varphi = \pi - \arccos(n_2 \cdot n_z) \tag{2}$$

The geometric relationship of the signs should be able to represent θ and φ . Then, the distribution of signs ought to enable us to find the parameters in formulas (1)(2). Therefore, we distribute the signs as that in Fig.5. Using lines to link all the points, we could obtain a simple model of the aircraft.

It is obvious that we could obtain the n_1 through the centers of each symmetrical sign pair. Adding the location information of sign 6 or 7, the vector n_2 is also known. Then, it becomes very easy for us to obtain the attitude of the planes through formula (1) and (2).

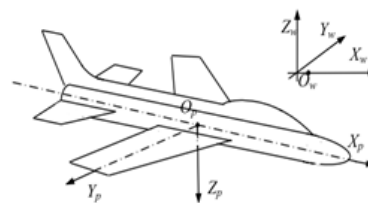


Figure 4 The Coordinates of aircraft

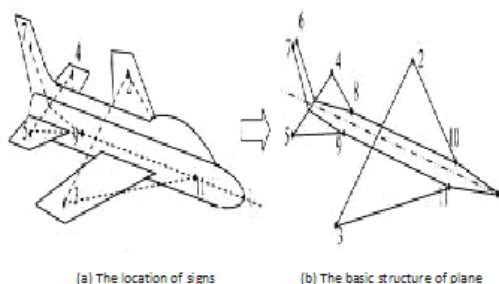


Figure 5 the Basic Structure Presented by Man-made Signs.

In common scenes, the minimum number of pixels for signs detection is about ten so that the algorithm could find out them correctly. In other words, the area occupied by designed signs in image should be large enough for computation. When we are designing the signs, some parameters should be computed so that all the signs could be found out correctly. The pixel number of the signs projection in image can be computed from the formula (3).

$$n \approx \frac{f \cdot x}{L \cdot dx} \times \frac{f \cdot y}{L \cdot dy} \tag{3}$$

Where dx and dy are the distance between two pixels in X-axis and Y-axis direction respectively. x and y are the maximum distance of signs in the directions which are parallel with the dx and dy. f is foci of the camera and L is the distance from camera to the light center. In terms of the minimum number of required pixels for detection, formula (3) helps us figure out the proper distance of the signs. In our aircraft measurement, the length of the plane body is 950mm. The length of wings is 1200mm while the width is approximately 150mm. The distance between cameras and plane is about 4 10m. Thus, we design the signs as follows (Tab.1).

During the measurement, the occlusion is unavoidable and we need to adjust the location in order to reduce probability of this situation to the minimum. Therefore, the distance between signs should be long enough, and better next to the edges of the aircraft. The attachment of these man-made signs is presented in Fig.6.

Table 1 The Distribution of the Man-made Signs on the Aircraft

Distribution	Types	Num	Main sizes
Aerofoil		4	d1=80mm,d2=15mm
Empennage		2	d1=60mm,d2=12mm
Vertical		4	d1=100mm,d2=12mm
Empennage			d3=28mm
Airframe side		4	d1=100mm,d2=12mm d3=30mm

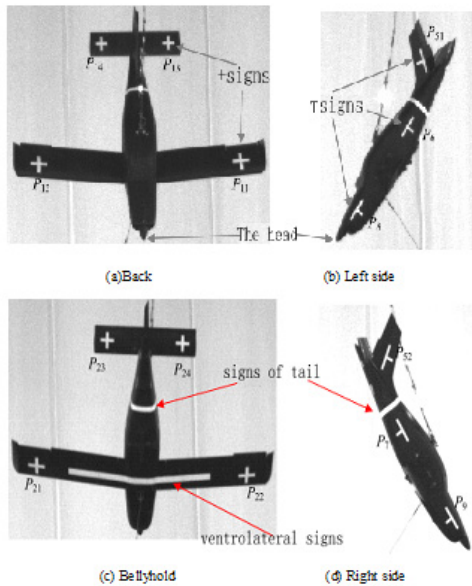


Figure 6 The Man-made Signs of the Aircraft.

3. THE ROLLING BALL DETECTION

Geometry estimation becomes a useful method to detect the signs in stereo matching [15], but many factors will change the signs character of linearity. For example, the projection of forane walking man in image is like a line with some distortions [16]. Since man-made signs in the image of aircraft spin measurement behave like stocky lines with deformation, traditional methods become hardly to meet precision requirement of recognition. Even though Davies [15] proposed a method to detect the small stocky lines that were insects in reality, it did not discuss how to deal with problem of lines distortion. In our experiment, there is an intersection in some of the man-made signs. To

ensure that we could detect the + ,T signs and not be disturbed by their cross point, the proposed algorithm should be able to span these intersections. Due to the characters of these signs, a novel detection method named rolling ball detection is proposed.

3.1. Detection for Stocky Lines

Even though the line (i.e. the man-made sign) may have deformation and a certain width, the centerline of it retains the character of beeline. A rolling ball whose diameter is equal to the width of line is used by the detection method for tracking the line in the image. It is noticeable that the trail of its center is almost a beeline (in Fig.7). Therefore, using this character, we can find the man-made signs exactly.

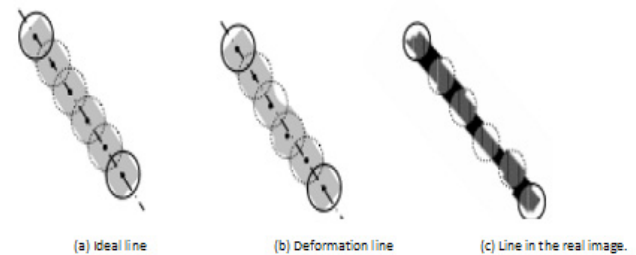


Figure 7 Theory of the rolling ball detection method.

First of all, we chose a matrix as the detecting window and design a coefficient for every pixel to transform the rectangular window to a rolling ball detection window (in Fig.8).

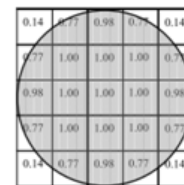


Figure 8 The rolling ball detection window in the 5 × 5 matrix.

In order to confirm the location of the starting point, the gray value is $g(i, j)$ and we assume that the $q(i, j) = 1 - g(i, j)$ is the weight of every pixel. The location of the center of weight in the window can be easily obtained by formula (4), where W is the detection window.

$$\begin{cases} x_w = \frac{\sum_{(i,j) \in W} i \cdot q(i,j)}{\sum_{(i,j) \in W} i \cdot n(i,j)} \\ y_w = \frac{\sum_{(i,j) \in W} j \cdot q(i,j)}{\sum_{(i,j) \in W} j \cdot n(i,j)}, \text{ when } (i,j) \in W, n(i,j)=1 \end{cases} \quad (4)$$

In most cases, the computed weight center cannot be exact integer. So we should round the results. The principle of this step is to find the nearest pixels location and regard it as revised weight center. The formula is as follows:

$$\begin{cases} u_c = u_g + 0.5 - rem(u_g + 0.5) \\ v_c = v_g + 0.5 - rem(v_g + 0.5) \end{cases} \quad (5)$$

$[u_g, v_g]$ is the raw computed result. rem is to take a remnant, and $[u_c, v_c]$ is a weight center.

Using the location difference between the geometrical center and weight center of the window, we can compute the moving direction and move the detection window to capture the starting point of the line (in Fig.9).

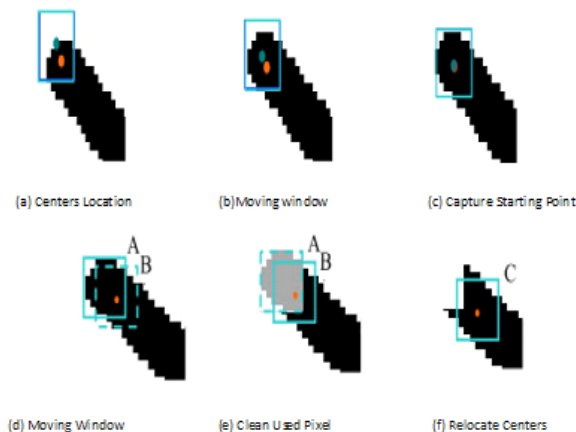


Figure 9 The process of capturing line tracking.

After capturing the starting point successfully, we zoom in the detection window so that we can obtain a new center of the window and a new center of weight (in Fig.9.b). A new location distance is generated during the process. In the following stage, we use it to find the moving direction to track the line (in Fig.9.d). To avoid the influence from the used pixel, when the window moves to the next location, we clean the gray value of the used pixel (in Fig.9.e). It is easy to find that when the detection window meets the end of the line, no matter how we enlarge the window, the distance between the window center and weight center will not change any longer or at least retains very small. In this situation, we could stop searching algorithm. Even though this method could help us find the potential signs, some other shapes may cause some errors during the detection. In order to avoid the effect of noise, we still need

to add some restrictions, stated as followings, so that we could detect the man-made signs correctly.

- The percentage of effective line points (line width) in detection window should be constant, and the computational formula (6) is used to get percentage of effective points.

$$\mu = \frac{n_e}{m^2} \times 100\%, \quad \text{inside} = \begin{cases} n_e = \sum_{p_{ij} > 0, p_{ij} \in W} n_{ij} \\ n_{ij} = \begin{cases} 1 & p_{ij} > 0 \\ 0 & p_{ij} = 0 \end{cases} \end{cases} \quad (6)$$

Where W is the field of detection window, p_{ij} is the gray of the pixels, n_e is the effective pixels in detection window, and m is the size of the detection window.

- The direction of extend vector should not change a lot. If the moving direction always changes, we regard this is curve, not the beeline.
- The moving steps of detection should be restricted in a particular range so that the detecting effects will not be affected by noise.

3.2. Intersection Traverse

The kernel of the rolling ball algorithm is using the offset between weight center and geometric center to move the detecting window. The intersection of signs will affect the moving direction, or even stop moving (in Fig.10). The case in Fig.10.c stops moving because offset is too small and the algorithm mistakes that it has reached the terminal. The case shown in Fig.10.d also stops moving due to the dramatic changes of moving direction. In order to detect the signs correctly, we should protect the algorithm from impact of these points.

One of the solution is that we can regard these signs are made up of short lines. However, this cannot be achieved in the experiment, as the length of them will be too short for detection. Therefore, our revised algorithm adds a new concept of direction weight and a condition of original orientation. That means in the optimal rolling ball detection method the moving direction is not only decided by the new computed moving direction.

In the Fig.11, n_1 represents the unit original moving direction. n_2 is the unit computed moving direction which is in terms of the difference between weight center and geometric center. n_3 is synthesized vector by and through formula(7).

$$n_3 = c_1 n_1 + c_2 n_2 \quad (7)$$

The c_1 and c_2 are weight coefficients. This determines the new detecting window 3. From the Fig.11, we can see that the offset of moving direction is declining by adding the restriction of original direction and this pulls the detecting window back to the right orientation.

Noticeably, there is mistiness in the definition of original vector. If we use the last moving vector as it, sometimes the offset is hard to be pulled back (Fig.13.a), or it causes a dramatic vibration in detection (Fig.13.b).

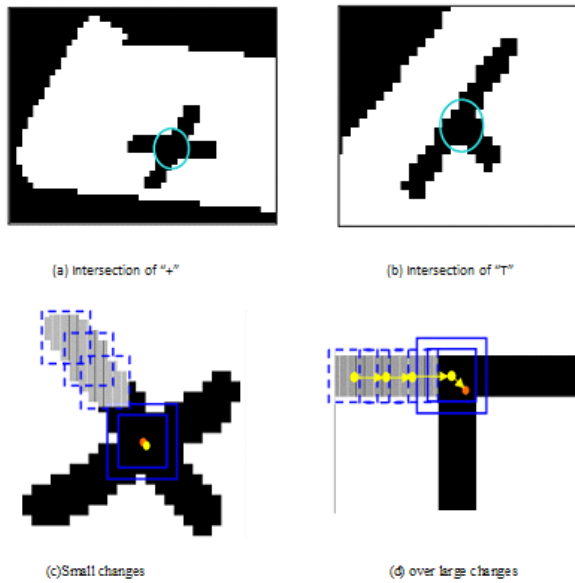


Figure 10 Effect of Intersection Area.

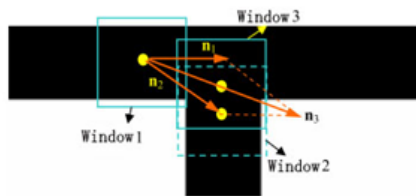


Figure 11 The Revised Moving Direction

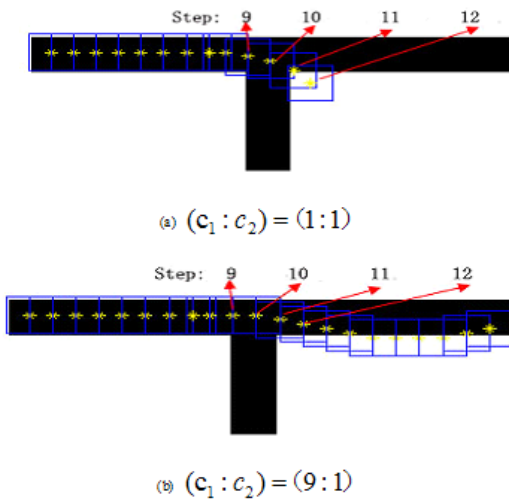


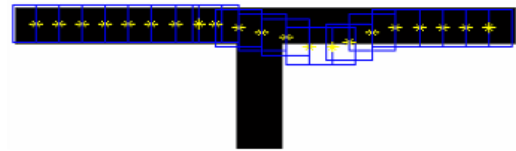
Figure 12 Synthesized vector n_3

In order to limit the intersection effect in other steps, we regard the summation of moving vectors in previous

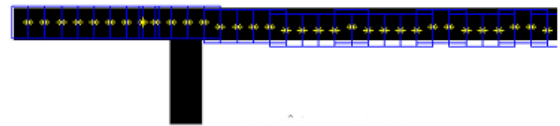
steps as original vector.

$$\begin{cases} n_1 = \sum_{i=1}^{x-1} n^{(i)} \\ n^{(x)} = n_3 = c_1 n_1 + c_2 n_2 \end{cases} \quad (8)$$

$n^{(i)}$ is the moving direction of detecting window. The original vector n_1 in x step is the summation of previous moving vectors. Using the new defined original vector n_1 . We could span the intersection without very little effect (in Fig.13).



(a) $(c_1 : c_2) = (1 : 1)$



(b) $(c_1 : c_2) = (9 : 1)$

Figure 13 n_1 is the summation of previous moving vectors

4. EXPERIMENTAL RESULTS AND ANALYSIS

In terms of the proposed method, we firstly use it in simulation to validate its usefulness in line detection. Then we capture the real scene images of aircraft measurement, and use the proposed method to detect the real signs.

4.1. Simulation Results

In our simulation, we firstly construct a picture with confused shapes and noise. Then the rolling ball algorithm is used to seek the line. In Fig.14(a), the method uses detection window to find out the starting points. Picture (b) shows the detecting results when the algorithm adds the restriction of the effective line points so that some other detected shapes have been eliminated. Using the vector restriction in (c), we confirm that all the detected shapes are linear. In terms of the moving step restriction, picture (d) gets the final detected results which are exactly what we want.

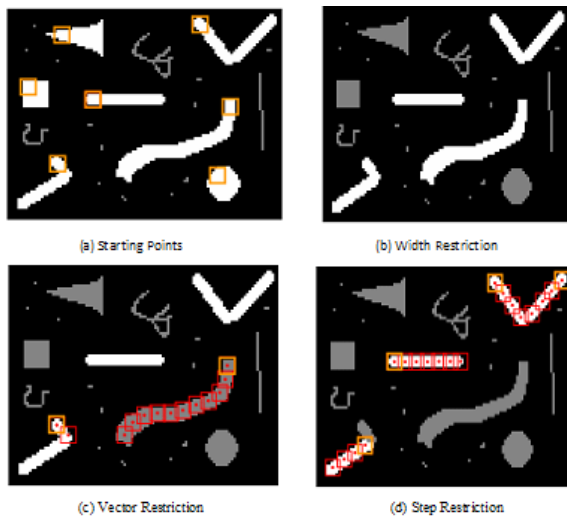


Figure 14 The Simulation of Rolling Ball Detection

4.2. Aircraft Experiment

We use this method to process the real images of aircraft measurement. During the processing, the rolling ball method is to detect the man-made signs for stereo matching. Firstly, we should confirm the suitable size of detecting window which will restrict the width of potential line. From the Tab.1, the + and T signs are very small, so we will open a 5×5 matrix as detecting window. Regarding the larger signs- on the bellyhold of the aircraft, the detecting window is a 7×7 matrix.

In the experiment, the restrictions of algorithm are efficient area, direction of vector, available steps. We detect the signs correctly in the Fig.15.

It is noticeable that, in the middle of the bellyhold lines, the directions of them have some changes. This is a common scene in the real detection experiment. In addition, as the scenarios are various, the thresholds of restrictions cannot be the same. Therefore, in order to adapt to these changes, we will loose some restrictions to ensure the efficiency of algorithm, and make this method be suitable for most cases.

Through numerous experiments in our provided scenes, we get some real data which could be used in signs detection for stereo matching (in Tab.2). All the data in it ensure the proposed algorithm to be capable of adapting to slight changes of scenes.

4.3. Error Analysis

In the Fig.15.c, we could find that when we are detecting the line, there is still a fluctuation in the centers track. This is because of the approximation error from formula(5). If we hope to decline the effect from it, we could enlarge the

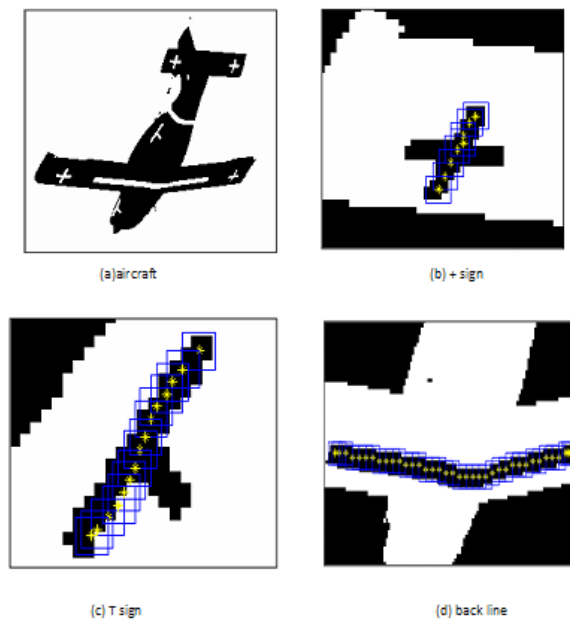


Figure 15 Rolling Ball Detection of Man-made Signs in Aircraft

Table 2 The Experimental Results of Rolling Ball Detection

Restriction	Efficient Pixels (percentage)			Vector Direction (degrees)			Length (steps)	
	u_{min}	Δu_{max}	Δu_m	Δa_m	da_m	S_{emin}	S_{emin}	
+ Signs	0.60	0.95	0.20	5	10	5	20	
T Signs	0.60	0.95	0.20	5	10	5	25	
Bellyhold Signs	0.50	0.90	0.25	10	15	40	80	

overall image matrix so that the precision of weight center computation could be improved. Another impact factor is the ratio of c_1 and c_2 . It decides the original vector and raw computed vectors influencing extent. If the ratio is quite large, it can span the intersection successfully. But once moving direction offsets, it is very difficult to pull it back to the right orientation. On the other hand, if the ratio is too small, intersection will cause failed detecting results. Therefore, the specific value is determined by the particular scenarios.

5. Conclusion

In this paper, we firstly provide several formulas to compute the attitude of the aircrafts. In terms of them, we design the proper man-made signs, including their shape, location, distribution to help us get the parameters of the aircraft. Then, a novel and reliable method, rolling ball detection, is proposed to seek these signs. The main idea in this method is to use the difference of the weight center and

geometrical center of each detecting window to track the signs. We propose three restrictions for algorithm to ensure the efficiency of it. Both of the computer simulation and aircraft measurement experiment in real scenario demonstrate that the algorithm could figure out the signs accurately. In addition, we get some useful data which could be regarded as basic data when adopt the rolling ball method to detect the signs.

Acknowledgement

This work was supported by the National Science Foundation of PR China under Grant Nos.60872151, 61003302, 61171136. We are grateful to all the reviewers for their insightful comments which improved the quality of the paper.

References

- [1] Zhu Ming-hong. *Free-spin test technique in 5m vertical wind tunnel in CARDC*. Journal of Experiments in Fluid Mechanics, 21, 9-53 (2007)
- [2] C. Michael Fremaux. Spin-tunnel investigation of a 1/28-scale model of the NASA F-18 High Alpha research vehicle (HARV) with and without vertical tails[R]. NASA contractor report, (1997)
- [3] John V. Foster, Kevin Cunningham, Charles M.Fremaux.Dynamics modeling and simulation of large transport airplanes in upset conditions[J].Navigation and control conference and exhibit, 15-18 (2005)
- [4] Walter L. Snow, Brooks A.Childers, Stephen B.Jones. Recent experiences with implementing a video based six degree of freedom measurement system for airplane models in a 20 foot diameter vertical spin tunnel[C]. Proceedings-SPIE the international society for optical. 1820, 158-180 (1992)
- [5] Hassan Mostafavi. Wind tunnel model aircraft attitude and motion analysis[J]. PRO.SPIE, Signal and image processing systems performance evaluation, simulation and modeling, 1483, 104-111 (1991)
- [6] M. R.Short,W. L. Snow. Videometric tracking of wind tunnel aerospace models at NASA Langley research center[C].the Thompson Symposium held at the University of York. 673-689 (1996)
- [7] Austin M. Murch, John V. Foster. Recent NASA research on aerodynamic modeling of post stall and spin dynamics of large transport airplanes[R]. AIAA Aerospace Sciences Meeting and Exhibit (2007) - ntrs.nasa.gov
- [8] Xi Qi-xin.*China built a vertical wind tunnel [OE/OL]*. <http://www.XINHUANET.com>, (2005)
- [9] Y.Domae, H.Takauji, S.Kaneko, T.Tanaka.*3D measurement of flexible objects by robust motion stereo*. SICE,2007 Annual Conference, 740-743 (2007)
- [10] Ali Erol, George Beis, Mircea Nicolescu,Richard D. Boyle, Xander Twombly. *Vision-based hand pose estimation:a review*. computer vision and image understanding, 108, 52-73 (2007)
- [11] Carlos D. Castillo, David W. *Using Stereo Matching with General Epipolar Geometry for 2D Face Recognition across Pose* ,Pattern Analysis and Machine Intelligence, 31, 2298-2304 (2009)
- [12] Danescu R. Nedeveschi, S. Meinecke, M.M Meinecke.*Lane Geometry Estimation in Urban Environments Using a Stereo vision System* Intelligent transportation systems conference, 10, 271-276 (2007)
- [13] Deva Ramanan, David A. Forsyth, Andrew Zisserman.*Tracking People by Learning Their Appearance*. IEEE Transaction on pattern analysis and machine intelligence, 26, 65 81 (2007)
- [14] Liang Lin, Ping Luo, Xiaowu Chen, *Kun Zeng Representing and recognizing objects with massive local image patches* ,Pattern Recognition, 45, 231C240 (2012)
- [15] E.R. Davies, M. Bateman, D.R. Mason, J.Chambers, C.Ridgway.*Design of efficient line segment detectors for ce-real grain inspection*. Pattern recognition letters, 24, 413-428 (2003)
- [16] Pan J S, Qiao Y L, Sun S H. *A fast k nearest-neighbours classification algorithm* IEICE Trans Fundamentals, 4, 961-963 (2004)



Luo Wusheng was born in 1972, and received the MSc degree and the PhD degree in instrumentation science from National University of Defense Technology, China, in 1997 and 2001, respectively. He is an assistant professor at the university. His research interests have focused on signal processing, instrumentation, and measurement tech-

niques.



Fanjiao Xiao was born in 1988, and received the MSc degree in instrument science from National University of Defense Technology, China, in 2010. She is a postgraduate student in NUDT. Her current research interests include sensor networks and image/video processing.



Lu Qin was born in 1980, and received the MSc degree and the PhD degree in instrumentation science from National University of Defense Technology, China, in 2004 and 2009, respectively. She is a lecturer in the Department of instrument science and technology, NUDT. Her current research interests include sensor networks, image/video processing and compression and embedded system design.



Li Pei was born in 1978, and received the MSc degree and the PhD degree in instrumentation science from National University of Defense Technology, China, in 2003 and 2010, respectively. Her current research interests include image/video processing and compression and wireless communication.